Electronic Supplementary Information

Experimental section

Materials: $Mn(NO_3)_2$ was purchased from Aladdin. $Ni(NO_3)_2 \cdot 6H_2O$, urea and Na_2S were purchased from Beijing Chemical Corp. (China). Pt/C (20 wt% Pt on Vulcan XC-72R) was purchased from Sigma-Aldrich. Nickel foam was provided by Suzhou District, Taili Metal Foam Business Factory. The ultrapure water used throughout all experiments through a Millipore system. All chemicals were used as received without further purification.

Preparation of precursor: Typically, $Ni(NO_3)_2 \cdot 6H_2O$ (0.291 g), $Mn(NO_3)_2$ (0.0358 g), and urea (0.60 g) were dissolved in 40 mL of deionized water under vigorous stirring for 15 min to form a clear solution. Then the solution was transferred to a 50 mL Teflon-lined stainless autoclave with a piece of cleaned nickel foam (2 × 3 cm). Then autoclave was sealed and heated to 120 °C for 6 h in an oven. After the autoclave cooled down to room temperature, the nickel foam was taken out and thoroughly washed with deionized water several times, then dried at 60 °C for 6 h in air. The Ni_3S_2/NF counterpart was made under the same conditions without using $Mn(NO_3)_2$. Other Mn-doped Ni_3S_2 samples were modulating the feed ratio of Mn and Ni salts as 1: 20, 2: 10 and 3: 10.

Preparation of Mn-Ni_3S_2/NF and Ni_3S_2/NF: In a typical procedure, Na_2S (0.593 g) was dissolved in 38 mL of deionized water under vigorous stirring. Then the Na_2S solution was transferred to a 50 mL Teflon-lined stainless autoclave with the corresponding precursor and the autoclave was maintained at 120 °C for 4 h. After the autoclave was cooled to room temperature, the sample was taken out and washed with deionized water several times, and dried at 60 °C for 4 h in air.

Preparation of Pt/C electrode: To prepare Pt/C electrode, 20 mg of Pt/C and 10 μL of Nafion solution (5 wt%) were dispersed in 1 mL of water/ethanol (v:v = 1:1) solvent to form a catalyst ink by sonication for 30 min. Then 70 μL of catalyst ink was loaded on bare nickel foam with a mass loading of 1.40 mg cm^{-2}.

Characterization: The X-ray diffraction (XRD) patterns were obtained from a LabX

XRD-6100 X-ray diffractometer with Cu Kα radiation (40 kV, 30 mA) of wavelength 0.154 nm (SHIMADZU, Japan). Scanning electron microscope (SEM) measurements were recorded on a XL30 ESEM FEG scanning electron microscope at an accelerating voltage of 20 kV. The structures of the samples were determined by Transmission electron microscopy (TEM) images on a HITACHI H-8100 electron microscopy (Hitachi, Tokyo, Japan) operated at 200 kV. X-ray photoelectron spectroscopy (XPS) data of the samples was collected on an ESCALABMK II x-ray photoelectron spectrometer using Mg as the exciting source. ICP-MS analysis was performed on a ThermoScientific iCAP6300.

Electrochemical measurement: The electrochemical measurements were performed on a CHI 660E electrochemical workstation (Chenhua, Shanghai). A three-electrode system was used in the experiment: a mercuric oxide electrode (Hg/HgO) was used as the reference electrode, a graphite rod was used as the counter electrode and the as-prepared Mn-Ni_3S_2/NF was used as the working electrode. All tests were carried out at room temperature. The potentials reported in this work were calibrated to reversible hydrogen electrode (RHE), using the following equation: E (RHE) = E (Hg/HgO) + 0.924 V. The electrochemical impedance spectroscopy (EIS) measurements were performed under a bias of -0.20 V vs RHE in the frequency ranging from 100 kHz to 10 mHz with an amplitude of 5 mV.

TOF calculations: The electrochemical active surface area (ECSA) is calculated using the following formula:[1]

$$A^{Mn-Ni_3S_2}_{ECSA} = \frac{C_{dl}}{40\ \mu F\ cm^{-2}\ per\ cm^2}_{ECSA}$$

To calculate the TOF, we used the following formula:[1,2]

$$TOF = \frac{\left(3.12 \times 10^{15} \times \frac{H_2/_S}{cm^2}\ per\ \frac{mA}{cm^2}\right) \times j}{1.761 \times 10^{15} \times A_{ECSA}}$$

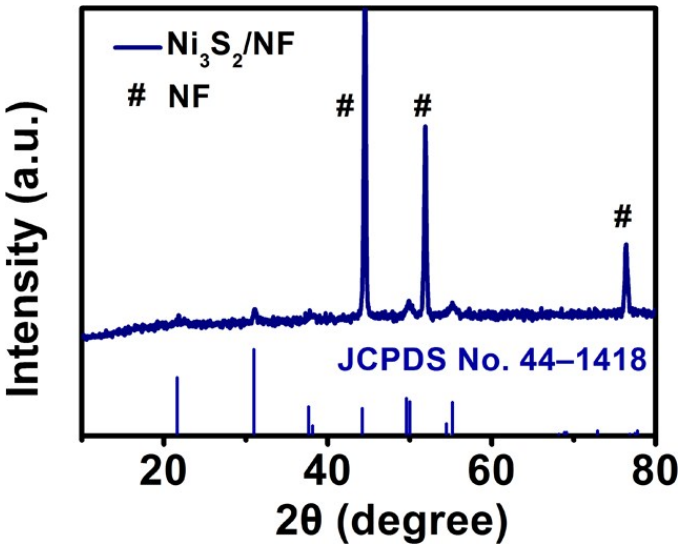

Fig. S1. XRD pattern of Ni_3S_2/NF.

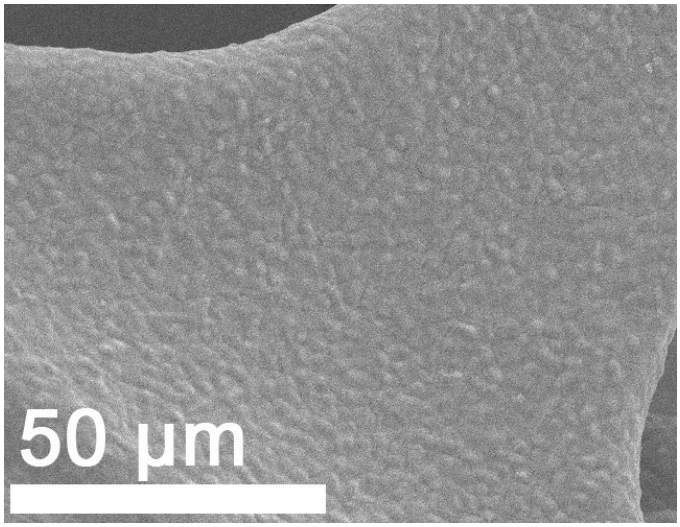

Fig. S2. SEM image of bare NF.

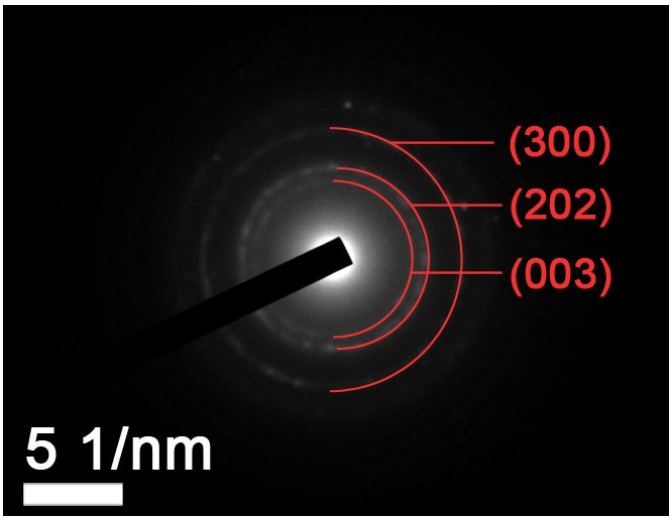

Fig. S3. SAED pattern taken from Mn-Ni_3S_2 nanosheet.

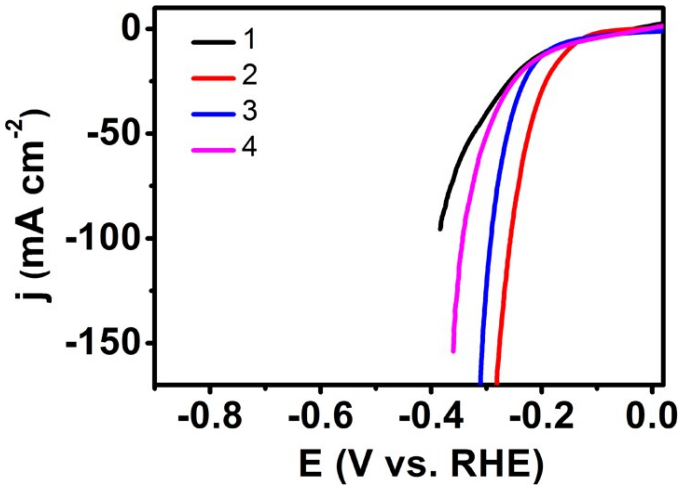

Fig. S4. LSV curves for Mn-Ni_3S_2/NF with different Mn doping degree: 3% (curve1), 5% (curve2), 9% (curve3) and 14% (curve4).

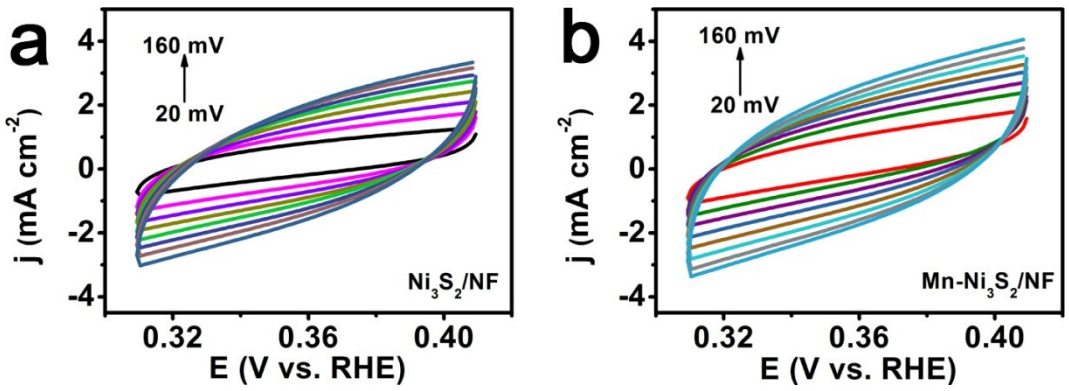

Fig. S5. CVs of (a) Ni_3S_2/NF and (b) Mn-Ni_3S_2/NF with various scan rates in the range between 0.31 and 0.41 V.

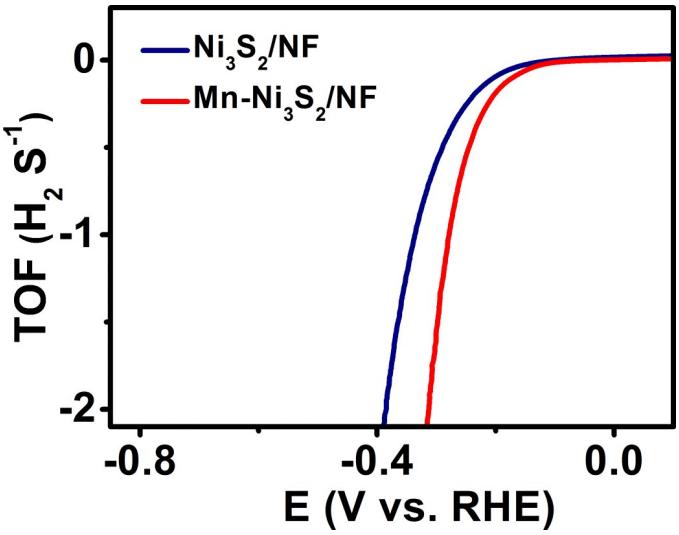

Fig. S6. TOF curve of Ni_3S_2/NF and Mn-Ni_3S_2/NF.

Table S1. Comparison of HER performance for Mn-Ni_3S_2/NF with other typical non-noble-metal electrocatalysts in 1.0 M KOH.

Catalyst	j (mA cm^{-2})	η (mV)	Ref.
Mn-Ni_3S_2/NF	10	152	This work
Ni_3S_2/NF	10	198	
Ni_3S_2	10	233	3
Ni_3S_2/AT-NF	10	200	4
V−Ni_3S_2−NW	10	~155	5
Ni_3S_2−NW	10	~199	6
$Fe_{0.1}$-NiS_2 NA/Ti	10	~200	7
Sn-Ni_3S_2/NF	10	137	8
Ni_3S_2/NF covered with RGO	10	157	9
Ni/NiS	10	230	10
N-Ni_3S_2/NF	10	155	11
$NiCo_2S_4$ NW/NF	10	210	12
MoS_2/Mo	10	184	13
$CoSe_2$/Carbon Cloth	10	190	14
CoS_2	10	~255	15
MoS_2	10	187	16

References

1 J. Kibsgaard, C. Tsai, K. Chan, J. D. Benck, J. K. Nørskov, F. Abild-Pedersen and T. F. Jaramillo, *Energy Environ. Sci*., 2015, **8**, 3022–3029.

2 H. Liang, A. N. Gandi, D. H. Anjum, X. Wang, U. Schwingenschlögl and H. N. Alshareef, *Nano lett.,* 2016, **16**, 7718–7725.

3 L. L. Feng, G. Yu, Y. Wu, G. D. Li, H. Li, Y. Sun and X. Zou, *J. Am. Chem. Soc.,* 2015, **137**, 14023–14026.

4 C. Ouyang, X. Wang, C. Wang, X. Zhang, J. Wu, Z. Ma, S. Dou and S. Wang, *Electrochim. Acta,* 2015, **174**, 297–301.

5 Y. Qu, M. Yang, J. Chai, Z. Tang, M. Shao, C. T. Kwok, M. Yang, Z. Wang, D. Chua, S. Wang, Z. Lu and H. Pan, *ACS Appl. Mater. Inter.,* 2017, **9**, 5959–5967.

6 J. Li, P. K. Shen and Z. Tian, *Int. J. Hydrogen Energy,* 2017, **42**, 7136–7142.

7 N. Yang, C. Tang, K. Wang, G. Du, A. M. Asiri and X. Sun, *Nano Res.,* 2016, **9**, 3346–3354.

8 J. Yu, F. Ma, Y. Du, P. Wang, C. Xu and L. Zhen, *ChemElectroChem.,* 2017, **4**, 594–600.

9 J. Lv, H. Miura, M. Yang and T. Liang, *Appl. Surf. Sci.,* 2017, **399**, 769–774.

10 G. Chen, T. Ma, Z. Liu, N. Li, Y. Su, K. Davey and S. Qiao, *Adv. Funct. Mater.,* 2016, **26**, 3314–3323.

11 T. Kou, T. Smart, B. Yao, I. Chen, D. Thota, Y. Ping and Y. Li, *Adv. Energy Mater.,* 2018, 1703538.

12 A. Sivanantham, P. Ganesan and S. Shanmugam, *Adv. Funct. Mater.,* 2016, **26**, 4661–4672.

13 Z. Pu, Q. Liu, A. M. Asiri, Y. Luo, X. Sun and Y. He, *Electrochim. Acta,* 2015, **168**, 133–138.

14 P. Chen, K. Xu, S. Tao, T. Zhou, Y. Tong, H. Ding, L. Zhang, W. Chu, C. Wu and Y. Xie, *Adv. Mater.,* 2016, **28**, 7527–7532.

15 H. Zhang, Y. Li, G. Zhang, P. Wan, T. Xu, X. Wu and X. Sun, *Electrochim.*

Acta, 2014, **148**, 170–174.

16 M. A. Lukowski, A. S. Daniel, F. Meng, A. Forticaux, L. Li and S. Jin, *J. Am. Chem. Soc.,* 2013, **135**, 10274–10277.